

Forcing Ferromagnetic Coupling Between Rare-Earth-Metal and 3d Ferromagnetic Films

Biplab Sanyal,^{1,*} Carolin Antoniak,² Till Burkert,¹ Bernhard Krumme,² Anne Warland,² Frank Stromberg,² Christian Praetorius,³ Kai Fauth,³ Heiko Wende,² and Olle Eriksson¹

¹*Department of Physics and Astronomy, Uppsala University, Box 516, SE-751 20 Uppsala, Sweden*

²*Faculty of Physics and Center for Nanointegration Duisburg-Essen (CeNIDE), University of Duisburg-Essen, Lotharstr. 1, 47048 Duisburg, Germany*

³*Faculty of Physics and Astronomy, University of Würzburg, Am Hubland, 97074 Würzburg, Germany*

(Received 6 December 2009; published 15 April 2010)

Using density functional calculations, we have studied the magnetic properties of nanocomposites composed of rare-earth-metal elements in contact with 3d transition metals (Fe and Cr). We demonstrate the possibility to obtain huge magnetic moments in such nanocomposites, of order $10\mu_B$ /rare-earth-metal atom, with a potential to reach the maximum magnetic moment of Fe-Co alloys at the top of the so-called Slater-Pauling curve. A first experimental proof of concept is given by thin-film synthesis of Fe/Gd and Fe/Cr/Gd nanocomposites, in combination with x-ray magnetic circular dichroism.

DOI: [10.1103/PhysRevLett.104.156402](https://doi.org/10.1103/PhysRevLett.104.156402)

PACS numbers: 71.20.Eh, 75.30.Cr, 75.50.Bb

Magnetic materials with a large saturation magnetic moment are used in various applications, such as write heads in computer hard disks, electromagnetic motors, generators, and transformers. Improved and more efficient materials are continuously sought after, but, for the last 75 years, the largest room temperature saturation moment ($2.45\mu_B$ /atom), as described by the maximum of the Slater-Pauling curve, has been provided by an $\text{Fe}_x\text{Co}_{1-x}$ ($x \sim 0.7$) alloy comprised of 3d transition metal elements [1]. Mn, with an atomic magnetic moment that in the dilute limit approaches $4\mu_B$ /atom in certain compounds, can be used in multilayers with Fe and Fe-Co alloys [2]. However, the magnetic coupling between Mn and Fe or Co provides antiparallel atomic moments, which reduce the net magnetic moment, and pure Mn does not order ferromagnetically.

Some experimental studies have proposed Fe_4N as a candidate material [3] for which the saturation moment per atom is suggested to be larger than that of Fe-Co alloys at the Slater-Pauling maximum (SPM), but several other reports contradict this finding [4]. Also, theoretical studies [5] showed that the addition of Mn to Fe_4N increases the unit cell volume and hence the magnetization, but the magnetic moment per atom was found not to exceed that of the Fe-Co alloys. Bergman *et al.* [6] found from their calculations that a high saturation magnetization can be obtained by a close packing of small Fe clusters in a Co matrix. This study was tied intimately to an experimental effort [7], but no definite conclusion was made about reaching a saturation moment at room temperature that is larger than that of the SPM.

In order to realize a combination of both large moment and high Curie temperature, we propose here multilayers of rare-earth-metal and 3d transition metals (nanolaminates). We verify our proposition by quantum mechanical

calculations, which have been proven to be extremely successful in reproducing the magnetic properties of materials. In addition to the theoretical work, we have also performed thin-film synthesis as well as element-specific measurements of the magnetism as a function of temperature, using the x-ray magnetic circular dichroism (XMCD) technique.

We will demonstrate here an avenue to provide ferromagnetic materials with large magnetic moments at room temperature by combining the large saturation moments of the rare-earth-metal atoms with the high critical temperatures of Fe or Co. In the past, multilayers composed of Fe and Gd have been studied [8], and it is encouraging to observe that thin layers of Gd in contact with Fe have a large atomic moment of the Gd atom, even at room temperature ($6.8\mu_B$ /atom). However, it is well known that magnetic 3d elements couple their spin moments antiferromagnetically to the spin moments of the rare-earth-metal atoms [9], and in the Fe/Gd multilayer [10], it was indeed found that the Fe and Gd moments couple in antiparallel alignment, resulting in a reduced magnetic moment.

We propose instead that one should consider monolayers (MLs) of rare-earth-metal ($R = \text{Gd}, \text{Tb}, \text{or Dy}$) elements on a film of Fe (or an Fe-Co alloy), separated by 1 ML of Cr. The combination $R/\text{Cr}/\text{Fe}$ has been chosen since it is known that rare-earth-metal moments couple antiferromagnetically with Cr [11,12], and Cr in turn couples antiferromagnetically with Fe [13]. Hence, an effective ferromagnetic coupling is expected between the rare-earth-metal and the Fe magnetic moments, as is shown schematically in Fig. 1. It is essential that this coupling is sufficiently strong to provide a large ordering temperature. We will show below that this is indeed true for the systems proposed here.

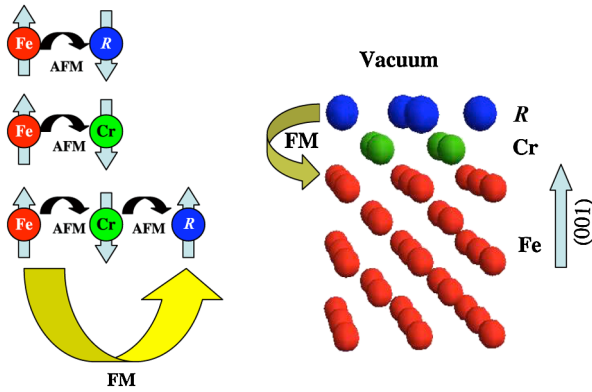


FIG. 1 (color online). Left: Schematic diagram of the magnetic interactions between the rare-earth-metal (R) and the $3d$ transition metals Fe and Cr. Right: Structure of the considered system.

Experimental evidence for ferromagnetic coupling between the R element and Fe is given by the analysis of the element-specific spin alignment by means of x-ray absorption spectroscopy and its associated XMCD presented in this work. As a prototype system, epitaxially grown nanocomposite layers of $\text{Gd}_{13}/\text{Cr}_n/\text{Fe}_{15}$ with different Cr interlayer thickness, n , was investigated. By means of RHEED measurements, it was controlled that the growth is epitaxial and that the Gd c axis is oriented in the film plane. Measurements at the Fe $L_{3,2}$ absorption edges in the energy range $680 \text{ eV} \leq E \leq 790 \text{ eV}$ and Gd $M_{5,4}$ absorption edges in the energy range $1150 \text{ eV} \leq E \leq 1280 \text{ eV}$ were performed in total electron yield (TEY) mode at the PM-3 bending magnet beam line at BESSYII synchrotron radiation source in magnetic remanence after saturation in fields of $\pm 3 \text{ T}$ under grazing x-ray incidence ($\theta = 70^\circ$ with respect to the sample normal). After each scan, either the helicity of x-ray photons or the direction of remanent sample magnetization was reversed. However, as discussed below, the increase of the magnetic ordering temperature of Gd necessary for large magnetic moments at room temperature depends on the coupling strength with Fe which is very sensitive to structural changes or diffusion processes.

The calculations were done by two different methods based on density functional theory. The VASP [14] plane wave code was used with the all-electron projector augmented wave method and the generalized gradient approximation to obtain the equilibrium interlayer separations along the stacking direction by minimizing the Hellman-Feynman forces. The kinetic energy cutoff was chosen to be 400 eV . The calculated equilibrium separation between the R and the Cr layer is 1.98 \AA , whereas it is 1.21 \AA between the Cr and the first Fe layer. At the fourth Fe layer, the value for bulk Fe ($\sim 1.43 \text{ \AA}$) is attained. Because of structural relaxations, the R atoms move outwards and the R -Cr interlayer distance becomes larger compared to that

of bulk Fe or Cr, whereas the Fe-Cr distance is reduced to a small degree.

The calculated equilibrium structure was then used to calculate the magnetic moments and interatomic exchange interactions by a fully relativistic implementation of the full-potential linear muffin tin orbitals (FP-LMTO) method [15]. A double basis was used to ensure a good convergence of the wave function. The $4f$ states of the rare-earth-metal atoms were treated as core states with the spin moments constrained to the values derived from Hund's rules, i.e., $m_s = 7\mu_B$ (Gd), $6\mu_B$ (Tb), and $5\mu_B$ (Dy).

In Fig. 2, we show the calculated layer-projected magnetic moments obtained from the FP-LMTO calculations. As the rare-earth-metal elements preserve their atomic spin and orbital moments of the strongly localized $4f$ shell [16], the orbital moments are easily evaluated and added to the calculated $4f$ spin moments [the orbital moments are $m_l = 0\mu_B$ (Gd), $3\mu_B$ (Tb), and $5\mu_B$ (Dy)]. We observe that the Fe and rare-earth-metal magnetic moments are aligned parallel to each other and the smaller Cr magnetic moment is aligned antiparallel to the Fe and R atoms, confirming our coupling scheme outlined in Fig. 1. It should be noted that the rare-earth-metal moment in this system is slightly larger than the corresponding atomic $4f$ moment, due to the fact that the $4f$ spin moment induces a magnetic moment in the conduction band. We also note that the Fe moment closest to the Cr atom is reduced compared to bulk Fe, whereas the other Fe atoms have a slightly enhanced magnetic moment.

We extended our study to include additional R layers in order to investigate the possible further enhancement of the magnetic properties. For 3 MLs of Dy, the average magnetic moment is calculated to be $3.68\mu_B/\text{atom}$; this average is obtained from 3 Dy, 1 Cr, and 3 Fe MLs from the Fe-Cr interface. The difference in the total energy of a ferromagnetic (FM) and an antiferromagnetic (AFM) ordering

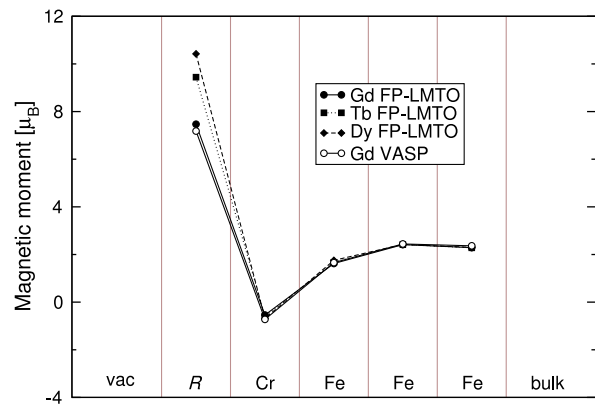


FIG. 2 (color online). Calculated layer-projected magnetic moments of the $R/\text{Cr}/\text{Fe}$ ($R = \text{Gd}, \text{Tb}, \text{and Dy}$) multilayers. The atomic orbital moments of the rare-earth-metal atoms were derived from Hund's rules and added to the calculated spin moments.

between the rare-earth-metal and Fe layers is a measure of the interatomic exchange interaction and hence provides an estimate of the Curie temperature. In Fig. 3, we present these values for the $R/\text{Cr}/\text{Fe}$ multilayers studied here. Again, it becomes clear that the rare-earth-metal and Fe magnetic moments prefer to align ferromagnetically, in accordance with the discussion around Fig. 1. We also calculated the energy of a configuration when half of the R atoms had their spins turned antiparallel to Fe, and the energy cost of this configuration was similar to the data shown in Fig. 3 (e.g., for a Dy layer, this energy is 110 meV/rare-earth-metal atom higher than the FM coupling). In addition, for the system with 3 Dy layers, the calculated exchange interaction between Dy and Fe was found to be 90 meV. The large values of these energy differences, of the order of 100 meV/rare-earth-metal atom, signify that the FM interaction between R atoms and Fe is strong and that the mean-field value of the Curie temperature is comparable to that of bulk Fe, i.e., of the order of 1000 K. Our results are in agreement with the study in Ref. [17] where the critical temperature of two atomic species that in elemental form have quite different ordering temperatures, one lower and one higher ordering temperature, was demonstrated to show ordering in a compound at the higher ordering temperature.

As a proof of concept of the proposed coupling scheme, the spin alignment was probed by means of XMCD for 13 MLs Gd coupled to 15 MLs Fe either directly as a reference sample for the well-known AFM coupling, or via 3, 4, or 5 MLs of Cr interlayer. Gd was used here as a representative R element, with an exchange coupling to the $3d$ film which is similar to that of Dy and Tb. Our experimental results are shown in Fig. 4. As expected, without Cr interlayer and for even numbers of MLs of Cr (data not shown), Gd couples antiferromagnetically to Fe moments. This behavior was also found for 3 MLs Cr, which is in

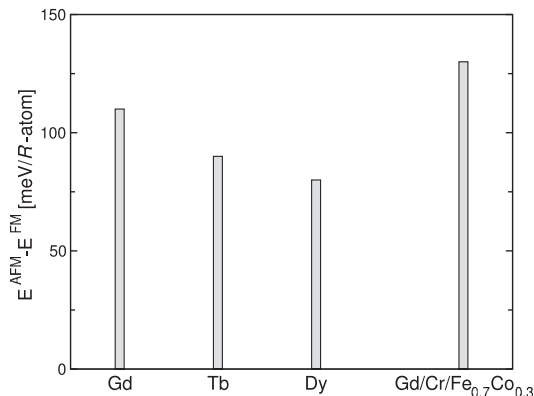


FIG. 3. Calculated total energy difference between an antiferromagnetic (AFM) and a ferromagnetic (FM) ordering within the rare-earth-element layer for $R/\text{Cr}/\text{Fe}$ ($R = \text{Gd}, \text{Tb}, \text{and Dy}$) and $\text{Gd}/\text{Cr}/\text{Fe}_{0.7}\text{Co}_{0.3}$.

contrast to what is expected from the scheme outlined in Fig. 1. It is possible that interface alloying between Cr and Fe over a few atomic layers distorts the coupling expected from Fig. 1, for thin Cr films. However, a FM coupling between Gd and Fe could be achieved for a 5 MLs Cr interlayer, which is clearly indicated by the ratio of the x-ray absorption signals with reversed direction of magnetization or reversed helicity of incident photons, $\mu + / \mu -$ as a function of photon energy (Fig. 4) [18]: The signal at the Gd M_5 absorption edge points down (<1), and at the M_4 edge it points up (>1) like Fe at its L_3 and L_2 edge, respectively.

The potential of using the suggested nanocomposites depends on their performance at room temperature, and hence the XMCD signal at the Gd $M_{5,4}$ absorption edges was measured at different temperatures between 11 and 300 K. As suggested in the literature [10,19], the experimental data was simulated by a simple model with an enhanced Curie temperature ($T_C^* \sim 1000$ K) of Gd in the interface region, as depicted in Fig. 4, due to the exchange coupling. The general trend of the temperature dependence of the Gd magnetization can be explained by the following model: For the directly coupled case (Fe/Gd), the thick-

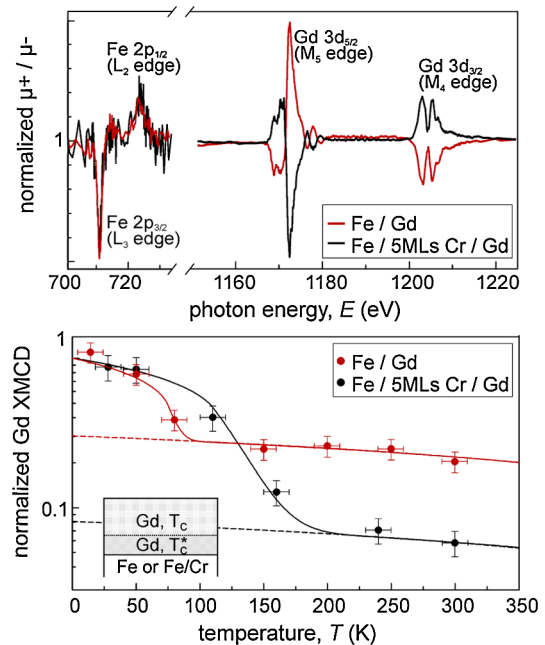


FIG. 4 (color online). Upper panel: XMCD measurements at the Fe $L_{3,2}$ and Gd $M_{5,4}$ absorption edges at $T = 11$ K in magnetic remanence exemplarily shown for the directly coupled Fe/Gd reference sample and the ferromagnetically coupled $\text{Gd}_{13}/\text{Cr}_5/\text{Fe}_{15}$ sample. Lower panel: Temperature dependence of XMCD at the Gd sites in an external magnetic field of ± 1 T. Experimental data are represented by symbols, solid lines representing a simulation assuming two regions with different Curie temperatures due to the coupling at the interface to Fe or Fe/Cr, respectively, as depicted in the inset. Contributions of the region with enhanced Curie temperature T_C^* are plotted by dashed lines.

ness of the interface regime of the Gd layer, where the Curie temperature T_C^* is enhanced, is the largest. Consequently, the inner part of the Gd film, where the Curie temperature is lower (it is actually reduced compared to bulk values due to finite-size effects), is thinnest for this system. Figure 4 also shows that the thicker the Cr interlayer becomes, the smaller is the effective coupling between Fe and Gd. Therefore, the thickness of the Gd interface region with enhanced ordering temperature is reduced. To analyze this simple model, we fitted the data in Fig. 4 according to the procedure described in Ref. [10]. In the case of the directly coupled Fe/Gd sample, the interface region with enhanced T_C corresponds to 4 MLs Gd. The remaining 9 MLs Gd exhibit a T_C of about 80 K. By introducing a Cr interlayer, the Gd interface region with enhanced T_C becomes smaller, i.e., 1 ML Gd interface for 5 MLs Cr. Our analysis suggests that the interface Gd region has a magnetic moment at room temperature, which is 70% ($5\mu_B/\text{atom}$) of the saturation moment at 0 K. Therefore, the thickness of the inner Gd part is 12 MLs connected to a T_C of 110 K. This value can be compared to the T_C of a 13 MLs thick Gd reference sample without Fe that was found to be around 120 K. The low T_C of the uncoupled Gd layers is the reason for the strong temperature dependence of the XMCD signal at low temperatures. The interface magnetism yields an additional contribution to the XMCD which is almost linear in the temperature range examined here. This leads to an XMCD signal at 300 K of about 20% of the saturation value for the Fe/Gd reference sample in good agreement to values reported in the literature [10,19]. The smaller, but clearly nonvanishing contribution in the case of the sample with 5 MLs Cr interlayer of about 6% proves the FM coupling between Fe and Gd.

We suggest here that R atoms in $R/\text{Cr}/\text{Fe}$ nanocomposite films may possess a large magnetic moment with ordering temperatures much above room temperature. In order to reach as big enhancement as possible, further improvements in the film growth must be achieved, in particular, any alloying between the Fe and Cr layers must be avoided so that ferromagnetic coupling between Fe and Gd can be reached for as thin Cr layers as possible, ideally 1 ML.

A further improvement of the desired magnetic properties is expected if Fe is replaced by an $\text{Fe}_{0.7}\text{Co}_{0.3}$ alloy. From our calculations for $\text{Gd}/\text{Cr}/\text{Fe}_{0.7}\text{Co}_{0.3}$, we find indeed an increase of the Fe-Co moments (Fig. 2), but it is not as pronounced as in bulk Fe-Co alloys. Furthermore, the antiparallel Cr moment is found to decrease, and the net effect is that the total magnetic moment of the $\text{Gd}/\text{Cr}/\text{Fe}_{0.7}\text{Co}_{0.3}$ system is considerably larger compared to the $\text{Gd}/\text{Cr}/\text{Fe}$ system. In addition, the interatomic exchange interaction becomes 20% larger than that of $\text{Gd}/\text{Cr}/\text{Fe}$, as can be seen in Fig. 3. Hence, both the low temperature saturation moment and the ordering tempera-

ture of the R layer is increased compared to the $\text{Gd}/\text{Cr}/\text{Fe}$ system.

Based on our experimental and theoretical work, we conclude that an optimal experimental realization of a high moment material would be a nanocomposite material, with a combination of magnetic materials which involves 1–3 layers of Dy separated by 1 Cr layer from 5–7 layers of an $\text{Fe}_{0.7}\text{Co}_{0.3}$ alloy. The experimental realization sets high demands on the thin-film growth by avoiding the alloying between Fe and Cr.

We gratefully acknowledge the BESSY II staff, especially T. Kachel and H. Pfau for their support. This work was funded by the Swedish Research Council (VR), STINT Institutional Grant for Young Researchers, Göran Gustafsson foundation, German Research Foundation (DFG) within the framework of SFB491, and the German Federal Ministry of Education and Research (BMBF, 05 ES3XBA/5). We also thank Swedish National Infrastructure for Computing for the allocation of supercomputer time. O. E. acknowledges support from ERC.

*Biplab.Sanyal@fysik.uu.se

- [1] P. Weiss and R. Forrer, *Ann. Phys. (Paris)* **12**, 279 (1929).
- [2] C. Cornea and D. Stoeffler, *J. Magn. Magn. Mater.* **198–199**, 282 (1999).
- [3] T. K. Kim and M. Takahashi, *Appl. Phys. Lett.* **20**, 492 (1972).
- [4] A. Sakuma, *J. Appl. Phys.* **79**, 5570 (1996).
- [5] M. S. Patwari and R. H. Victora, *Phys. Rev. B* **64**, 214417 (2001).
- [6] A. Bergman *et al.*, *Phys. Rev. B* **70**, 174446 (2004).
- [7] C. Binns, *Surf. Sci. Rep.* **44**, 1 (2001).
- [8] N. I. N. Hosoito and H. Hashizume, *J. Phys. Condens. Matter* **14**, 5289 (2002).
- [9] B. Spunzar and B. Kozarzewski, *Phys. Status Solidi B* **82**, 205 (1977).
- [10] D. Haskel *et al.*, *Phys. Rev. Lett.* **87**, 207201 (2001).
- [11] M. Loewenhaupt *et al.*, *J. Magn. Magn. Mater.* **121**, 173 (1993).
- [12] Y. Li *et al.*, *Physica B (Amsterdam)* **234–236**, 489 (1997).
- [13] S. Mirbt *et al.*, *Solid State Commun.* **88**, 331 (1993).
- [14] G. Kresse and J. Hafner, *Phys. Rev. B* **47**, R558 (1993); G. Kresse and J. Furthmüller, *Phys. Rev. B* **54**, 11169 (1996).
- [15] J. M. Wills *et al.*, in *Electronic Structure and Physical Properties of Solids: The Uses of The LMTO Method* (Springer, Berlin, 2000), pp. 148–167.
- [16] C. Kittel, *Introduction to Solid State Physics* (John Wiley & Sons, New York, 1996), 7th ed.
- [17] R. Skomski and D. Sellmyer, *J. Appl. Phys.* **87**, 4756 (2000).
- [18] Plotting of the quotient was favored over the difference between $\mu+$ and $\mu-$ spectra that is mostly presented in literature since it easily suppresses the strong background signal at the Fe absorption edges under grazing incidence caused by the sample configuration (Fe screened by Cr, Gd, and the cap layer).
- [19] Y. Choi *et al.*, *Phys. Rev. B* **70**, 134420 (2004).